

Published in final edited form as:

Circ Res. 2004 August 6; 95(3): 292–299. doi:10.1161/01.RES.0000136817.28691.2d.

## Partial Inhibition of Sodium/Calcium Exchange Restores Cellular Calcium Handling in Canine Heart Failure

Ion A. Hobai, Christoph Maack, and Brian O'Rourke

Johns Hopkins University Institute of Molecular Cardiobiology, Department of Medicine, Baltimore, Md.

### Abstract

Sodium/calcium ( $\text{Na}^+/\text{Ca}^{2+}$ ) exchange (NCX) overexpression is common to human heart failure and heart failure in many animal models, but its specific contribution to the cellular  $\text{Ca}^{2+}$  ( $[\text{Ca}^{2+}]_i$ ) handling deficit is unclear. Here, we investigate the effects of exchange inhibitory peptide (XIP) on  $\text{Ca}^{2+}$  handling in myocytes isolated from canine tachycardic pacing-induced failing hearts. Whole-cell patch-clamped left ventricular myocytes from failing hearts (F) showed a 52% decrease in steady-state sarcoplasmic reticulum (SR)  $\text{Ca}^{2+}$  load and a 44% reduction in the amplitude of the  $[\text{Ca}^{2+}]_i$  transient, as compared with myocytes from normal hearts (N). Intracellular application of XIP (30  $\mu\text{mol/L}$ ) normalized the  $[\text{Ca}^{2+}]_i$  transient amplitude in F (3.86-fold increase), concomitant with a similar increase in SR  $\text{Ca}^{2+}$  load. The degree of NCX inhibition at this concentration of XIP was  $\approx 27\%$  and was selective for NCX: L-type  $\text{Ca}^{2+}$  currents and plasmalemmal  $\text{Ca}^{2+}$  pumps were not affected. XIP also indirectly improved the rate of  $[\text{Ca}^{2+}]_i$  removal at steady-state, secondary to  $\text{Ca}^{2+}$ -dependent activation of SR  $\text{Ca}^{2+}$  uptake. The findings indicate that in the failing heart cell, NCX inhibition can improve SR  $\text{Ca}^{2+}$  load by shifting the balance of  $\text{Ca}^{2+}$  fluxes away from transsarcolemmal efflux toward SR accumulation. Hence, inhibition of the  $\text{Ca}^{2+}$  efflux mode of the exchanger could potentially be an effective therapeutic strategy for improving contractility in congestive heart failure.

### Keywords

exchange inhibitor peptide; XIP; excitation–contraction coupling; calcium transient

Altered calcium ( $\text{Ca}^{2+}$ ) handling is a key factor in the pathophysiology of heart failure. A typical failing heart cell shows a decrease in the ability of the internal stores (the sarcoplasmic reticulum [SR]) to load with  $\text{Ca}^{2+}$ , and an increase in  $\text{Ca}^{2+}$  extrusion from the cell by the sodium/calcium exchanger (NCX). NCX overexpression is a component of altered  $\text{Ca}^{2+}$  handling in human<sup>1</sup> and animal models,<sup>2,3</sup> but it is unclear whether it is compensatory or contributes to dysfunction. One widely held hypothesis is that NCX overexpression compensates for decreased  $\text{Ca}^{2+}$  reuptake into the SR by increasing  $\text{Ca}^{2+}$  extrusion from the cell,<sup>4,5</sup> which improves relaxation (positive lusitropic) but at the cost of a further depletion of SR  $\text{Ca}^{2+}$  stores (negative inotropic). Further complicating the issue is the observation that NCX overexpression is also found in hypercontractile models with no SR dysfunction.<sup>6</sup>

We studied the effect of partially correcting the NCX overexpression (by applying an exchange inhibitory peptide [XIP]) in a canine model of heart failure. Partial inhibition of NCX

normalized both SR  $\text{Ca}^{2+}$  release and re-uptake, arguing for a critical role for NCX overexpression in the  $\text{Ca}^{2+}$  handling deficit as well as for its potential as a therapeutic target.

## Materials and Methods

These experiments were performed using a canine tachycardic pacing-induced heart failure model. We,<sup>2,7,8</sup> and others,<sup>9</sup> have previously demonstrated that this animal model reproduces a remarkable number of features of the human disease. Induction of heart failure, isolation of midmyocardial cardiomyocytes, single-cell electrophysiology studies, and  $\text{Ca}^{2+}$  measurements were performed (at 37°C) as previously described,<sup>2</sup> and as summarized in the expanded Methods section in the online data supplement available at <http://circres.ahajournals.org>.

### Excitation–Contraction Coupling Experiments

The main experimental protocol (Figures 1 through 5) consisted of a train of 0.5-second depolarizations from  $-80\text{mV}$  to  $+10\text{mV}$ , applied at 0.5 Hz until steady-state, followed by a rapid application of caffeine to measure SR  $\text{Ca}^{2+}$  load. The external solution contained (mmol/L): NaCl 140; KCl 4;  $\text{CaCl}_2$  2;  $\text{MgCl}_2$  1, HEPES 5; Glucose 10; niflumic acid 0.1 (to block  $\text{Ca}^{2+}$ -activated  $\text{Cl}^-$  currents), pH 7.4. After reaching steady-state, 30  $\mu\text{mol/L}$  tetrodotoxin ( $\text{Na}^+$  channel blocker) was applied, to allow a better estimation of the peak of the L-type  $\text{Ca}^{2+}$  current ( $I_{\text{Ca,L}}$ ). For the experiment shown in Figure 6e through 6g, the solution had  $\text{Na}^+$  and  $\text{Ca}^{2+}$  replaced with  $\text{Li}^+$  and  $\text{Ni}^{2+}$ , and was  $\text{K}^+$ -free. Superfusing solutions were rapidly changed using a solenoid-controlled heated switching device.<sup>2</sup> The pipette solution contained (in mmol/L): K glutamate 125; KCl 19;  $\text{MgCl}_2$  0.5; MgATP 5; NaCl 10; HEPES 10; pH 7.25; and 50  $\mu\text{mol/L}$  indo-1 (pentasodium salt, Calbiochem). The liquid junction potential between the pipette and bath was corrected post hoc.

### NCX Measurement With $[\text{Ca}^{2+}]_i$ Buffer

In Figure 6a, the NCX current was measured selectively as described previously.<sup>2</sup> The external solution was  $\text{K}^+$ -free (to block the inward rectifier  $\text{K}^+$  current and the  $\text{Na}^+/\text{K}^+$  pump) and also contained 100  $\mu\text{mol/L}$  niflumic acid, 10  $\mu\text{mol/L}$  strophanthidin ( $\text{Na}^+/\text{K}^+$  pump inhibitor), and 10  $\mu\text{mol/L}$  nitrendipine (dihydropyridine antagonist). The intracellular (pipette) solution contained (mmol/L): CsCl 110; NaCl 20;  $\text{MgCl}_2$  0.4; MgATP 5; glucose 5; HEPES 5;  $\text{CaCl}_2$  1.75; and BAPTA 5. The mixture of BAPTA and  $\text{Ca}^{2+}$  gave a free  $[\text{Ca}^{2+}]_i$  of 112 nmol/L (WinMaxC, Ver. 2.4; Chris Patton, Stanford University, Calif).

### XIP Synthesis

XIP (RLLFYKYVYKRYRAGKQRG) was synthesized by the Biosynthesis and Sequencing Facility, Department of Biological Chemistry, Johns Hopkins University, kept as 20 mmol/L stock in ethanol and added to the pipette solution (control experiments had equivalent amount of ethanol added, which had no effect on the parameters measured).

We did not observe any time-dependence of the effect of XIP, which reached steady-state as soon as we started recording (2 to 7 minutes from achieving the whole cell mode, at which time the indo-1 signal had reached a steady level).

Statistics shown are mean $\pm$ SEM, with  $P < 0.05$  as the criterion for statistical significance.

## Results

Because there is currently no selective, externally applicable inhibitor of NCX (available compounds<sup>10,11</sup> or inorganic blocking cations<sup>12</sup> are either nonselective<sup>11,13</sup> or preferentially block reverse-mode exchange<sup>10</sup>), we compared cellular responses in the absence and presence

of exchange inhibitor peptide<sup>14</sup> (XIP), added directly to the intracellular solution. XIP has been shown to be an effective NCX inhibitor under various conditions.<sup>12,14,15</sup>

### Effect of XIP on Steady-State $[Ca^{2+}]_i$ Transients

Cardiac cells isolated from normal (N) or failing (F) hearts were subjected to trains of depolarizations to assess the main mechanisms of  $Ca^{2+}$ -induced  $Ca^{2+}$  release (CICR), ie, trigger  $Ca^{2+}$  entry through L-type  $Ca^{2+}$  channels ( $I_{Ca,L}$ ), the rate of rise ( $\Delta Ca/\Delta t$ ) and amplitude ( $\Delta Ca$ ) of the  $[Ca^{2+}]_i$  transient, and the SR  $Ca^{2+}$  load ( $Ca_{SR}$ , measured as the integral of NCX current during caffeine application,<sup>2</sup> see later; Figure 1). Myocytes from failing hearts cells showed the characteristic  $Ca^{2+}$  handling deficit, with decreased  $[Ca^{2+}]_i$  transients and  $Ca_{SR}$ , and no change in  $I_{Ca,L}$  (Figures 1 and 2). Internal equilibration with 10  $\mu\text{mol/L}$  XIP induced a large increase in the steady-state  $Ca_{SR}$  and  $[Ca^{2+}]_i$  transients, without any effect on  $I_{Ca,L}$  (Figures 1 and 2). A small increase in  $Ca_{SR}$  was also seen in normal myocytes. At a concentration of 30  $\mu\text{mol/L}$ , an additional increase in  $\Delta Ca$  was observed in both groups. In failing cells,  $\Delta Ca$  was increased 3.86-fold by XIP compared with the untreated group (Figure 2c). Importantly, and somewhat unexpectedly, the enhancement of excitation–contraction coupling occurred without a significant change in diastolic  $[Ca^{2+}]_i$  (see later).

### Effect of XIP on the $[Ca^{2+}]_i$ Staircase

Immediately after a caffeine-induced  $Ca^{2+}$  release (which unloads the SR completely<sup>2</sup> and thus gives a similar starting point in all groups), repetitive square wave depolarizations induced a gradual increase in the  $[Ca^{2+}]_i$  transient (positive staircase or “treppe”) in N, as a consequence of SR  $Ca^{2+}$  loading. XIP slightly accelerated the pulse-dependent  $[Ca^{2+}]_i$  increase for the first 10 pulses (Figure 3), which, after 20 to 30 pulses, led to the increased steady-state values shown in Figures 1 and 2. The positive staircase was characteristically absent in untreated F, but was fully restored with the addition of 10 or 30  $\mu\text{mol/L}$  XIP (Figure 3b). Again, the increase in the amplitude of the  $[Ca^{2+}]_i$  transient was associated with a maintained or slightly decreased diastolic  $[Ca^{2+}]_i$  (Figure 3c and 3d).

### Effect of XIP on $[Ca^{2+}]_i$ Decay

Because NCX is a major  $Ca^{2+}$  removal mechanism, especially in myocytes from failing hearts, we anticipated that XIP might decrease the rate of diastolic  $Ca^{2+}$  decay and adversely affect cell relaxation. However, the results indicated the contrary: at steady-state, the time constant of decay of  $[Ca^{2+}]_i$  on repolarization to the holding potential ( $\tau_{Ca}$ ; representing here the combined NCX and SERCA actions) was accelerated by XIP in both groups (Figure 4a). This indicated that NCX inhibition may be associated with an unexpected increase in the rate of SR  $Ca^{2+}$  uptake (which was also consistent with the large increase in  $Ca_{SR}$ ).

On closer inspection,  $\tau_{Ca}$  acceleration proved to be dependent not directly on XIP, but was secondary to the increase in  $[Ca^{2+}]_i$  (Figure 4b). In normal cells, during the development of the  $Ca^{2+}$  staircase (as in Figure 3), the increase in peak  $[Ca^{2+}]_i$  was reproducibly associated with an acceleration of  $\tau_{Ca}$  (Figure 4c, white circles). A similar effect was previously reported by Schouten et al<sup>16</sup> and attributed to SERCA activation (because it was sensitive to thapsigargin<sup>17</sup>). The same relationship was found in failing cells, when the staircase was recovered in the presence of XIP (eg, Figure 4b for typical traces; Figure 4c, black circles for average data). Finally, clearly demonstrating that the acceleration of  $Ca_i$  decay was not caused by XIP in itself, we could reproduce the effect in F when the  $[Ca^{2+}]_i$  transients were enhanced by an increase in external  $Ca^{2+}$  concentration, in the absence of XIP (Figure 4c, black diamonds).

Therefore, we conclude that NCX inhibition, by decreasing  $Ca^{2+}$  extrusion, induced an increase in cytosolic  $Ca^{2+}_i$ , which had the effect of stimulating SERCA. Both NCX inhibition and the

indirect SERCA stimulation were responsible for the full magnitude of the inotropic effect. This occurred with the maintenance (and even improvement) of relaxation in F in the presence of XIP (see Discussion).

### Quantification of NCX Inhibition

The large positive inotropic effect of 10 and 30  $\mu\text{mol/L}$  XIP in F required an estimation of the actual degree of NCX inhibition obtained with these concentrations.

Because NCX is the major  $\text{Ca}^{2+}$  transporter during caffeine-induced  $\text{Ca}^{2+}$  release, the time constant of  $[\text{Ca}^{2+}]_i$  decay ( $\tau_{\text{Ca}}$ ) in the presence of caffeine is a measure of NCX activity (Figure 1). However, we were unable to show a significant effect on  $\tau_{\text{Ca}}$  for caffeine-induced  $\text{Ca}^{2+}$  transients with 30  $\mu\text{mol/L}$  XIP (Figure 5a). An alternative measure of NCX activity in these experiments is the amplitude of the inward NCX current, plotted as a function of  $[\text{Ca}^{2+}]_i$ . This relation was also not significantly reduced by 30  $\mu\text{mol/L}$  XIP in either group (Figure 5b; n values: N, 5/6; N +30XIP, 9/5; F, 4/3; F +30XIP, 3/3; failing group data not shown). Because XIP has been demonstrated to be an effective NCX inhibitor under various conditions,<sup>12,14,15</sup> we hypothesized that the specific conditions associated with the caffeine experiments may have masked the inhibitory effect (see Discussion). Therefore, we persisted in investigating this question by performing 2 additional experiments.

In the first, we measured NCX activity as the  $\text{Ni}^{2+}$ -sensitive current elicited by depolarizations from  $-40\text{mV}$  to various potentials (as described<sup>2</sup>). Consistent with previous results,<sup>12</sup> in these conditions, 30  $\mu\text{mol/L}$  XIP inhibited NCX by  $\approx 67\%$  (at  $+80\text{mV}$ , Figure 6a and 6b) in both N and F, and the block was mode-independent.

We also estimated the degree of NCX inhibition in the minimally  $\text{Ca}^{2+}$ -buffered conditions that were used for the excitation–contraction coupling experiments shown in Figures 1 through 3. With SR  $\text{Ca}^{2+}$  uptake (and, thus, indirectly,  $\text{Ca}^{2+}$  release) blocked by thapsigargin, membrane depolarizations from  $-80$  to  $+100\text{mV}$  elicited reverse-mode NCX-mediated  $[\text{Ca}^{2+}]_i$  increases (Figure 6c and 6d). Under these conditions, 10 and 30  $\mu\text{mol/L}$  XIP induced 23% and 27% NCX inhibition, respectively (Figure 6c and 6d).

### Selectivity of NCX Inhibition

XIP has been reported to inhibit both the sarcolemmal and SR  $\text{Ca}^{2+}$  pumps in vitro.<sup>18</sup> Therefore, it was important to establish that reversal of the failing phenotype was caused by a selective effect on NCX. In the same experimental conditions as for Figures 1 through 5, the time constants of  $[\text{Ca}^{2+}]_i$  decay attributable to the SR  $\text{Ca}^{2+}$  pump and other, slower, mechanisms (including the plasmalemmal  $\text{Ca}^{2+}$  ATPase, PMCA, and mitochondrial  $\text{Ca}^{2+}$  uptake) were assessed using caffeine applications in  $\text{Na}^+$ -free and  $\text{Ca}^{2+}$ -free solution<sup>19</sup> (see Figure 6); 30  $\mu\text{mol/L}$  XIP did not inhibit either transporter (Figure 6e and 6g). The previously reported sensitivity of the pumps to XIP was not observed here, likely because of differences in the experimental conditions. For example, Enyedi et al<sup>18</sup> measured PMCA and SERCA in isolated membrane vesicles from rabbit erythrocyte and skeletal muscle preparations, respectively, and after proteolytic activation of PMCA.

### Modulation by the Membrane Potential

The present experiments were designed to assess  $\text{Ca}^{2+}$ -induced  $\text{Ca}^{2+}$  release at the maximum  $\text{Ca}^{2+}$  current ( $I_{\text{Ca,L}}$ ) amplitude. However, an action potential-driven  $\text{Ca}_i$  transient would likely include a component of  $\text{Ca}^{2+}$  entry through the NCX, which is larger in F than in N.<sup>20,21</sup> Therefore, it was of interest to determine if the positive inotropic effect of XIP was also evident in F during trains of action potentials in current clamp conditions. Figure 7a and 7b show that action potential-triggered  $\text{Ca}^{2+}$  transients in F were significantly smaller than in N, and were

significantly increased by 30  $\mu\text{mol/L}$  XIP. In N, 30  $\mu\text{mol/L}$  XIP also tended to increase the  $\text{Ca}^{2+}$  transient amplitude, but the effect did not reach statistical significance.

### Modulation by Pacing Frequency

Increased pacing frequencies are usually associated with an increase in diastolic  $[\text{Ca}^{2+}]_i$ , because of the decrease in the diastolic interval; therefore, we tested whether NCX inhibition might exacerbate this increase. Figure 7c confirms that this was not the case. F groups treated with 30  $\mu\text{mol/L}$  XIP (n=4/2) had similar diastolic  $[\text{Ca}^{2+}]_i$  levels, as compared with untreated N (n=5/2) when stimulated at frequencies between 0.5 and 3 Hz. The increase in steady-state peak systolic  $[\text{Ca}^{2+}]_i$  was maximal between 1 and 2 Hz.

## Discussion

### Effect of NCX Inhibition in Normal Canine Cells

To maintain  $\text{Ca}^{2+}$  balance at steady-state, cellular  $\text{Ca}^{2+}$  extrusion via forward-mode NCX must match  $\text{Ca}^{2+}$  entry via  $I_{\text{Ca,L}}$  and reverse-mode NCX.<sup>22</sup> It follows that, for the whole cardiac cycle, the net effect of NCX must be  $\text{Ca}^{2+}$  removal (ie, forward-mode NCX must be larger than reverse-mode NCX), and partial inhibition of NCX must lead to cellular  $\text{Ca}^{2+}$  accumulation unless  $\text{Ca}^{2+}$  influx also declines in parallel. The increase in SR  $\text{Ca}^{2+}$  load and the subsequent increase in the amplitude of the  $\text{Ca}^{2+}$  transient has the dual effect of inhibiting  $\text{Ca}^{2+}$  entry via  $\text{Ca}^{2+}$ -dependent inactivation of  $I_{\text{Ca,L}}$  (Figure 4b) and increasing  $\text{Ca}^{2+}$  efflux through NCX through the remaining unblocked exchangers. A new steady-state is thus reached, characterized by increased  $[\text{Ca}^{2+}]_i$  levels, so that NCX  $\text{Ca}^{2+}$  extrusion equals again  $\text{Ca}^{2+}$  influx. Consistently, in the present experiments, 27% inhibition of NCX induced an 80% increase in the amplitude of the  $[\text{Ca}^{2+}]_i$  transients in N (at 0.5 Hz;  $P=0.02$ ).

### Frequency-Dependent Acceleration of Relaxation

The absence of an increase in diastolic  $\text{Ca}^{2+}$  with XIP was, however, notable. One would have predicted that inhibiting  $\text{Ca}^{2+}$  extrusion would lead to slowed relaxation and an increase in diastolic steady-state  $[\text{Ca}^{2+}]_i$ . This was, a priori, an argument against the use of NCX inhibitors in heart failure. Serendipitously, we observed the opposite effect, as a consequence of indirect  $[\text{Ca}^{2+}]_i$ -dependent stimulation of SR  $\text{Ca}^{2+}$  uptake.

$\text{Ca}^{2+}$ -mediated SERCA activation was first described by Schouten in 1990<sup>16</sup> and later coined “frequency-dependent acceleration of relaxation.”<sup>23</sup> Although partial acceleration of SR  $\text{Ca}^{2+}$  uptake at high  $\text{Ca}^{2+}$  is expected because of the sigmoidal dependence of the transport kinetics on the concentration of the substrate,<sup>17</sup> an additional activation has been ascribed to an allosteric regulatory mechanism. The nature of the  $[\text{Ca}^{2+}]_i$ -sensitive mediator is still unclear: a possible mechanism suggested by some,<sup>17</sup> but not all,<sup>24</sup> studies was calmodulin-dependent phosphorylation. Regardless of the mechanistic details,  $[\text{Ca}^{2+}]_i$ -mediated SERCA activation represents an effective autoregulatory mechanism that protects against cytosolic  $[\text{Ca}^{2+}]_i$  overload. It is also a positive feedback mechanism in which increased SR  $\text{Ca}^{2+}$  release and uptake potentiate each other, a likely explanation for the large inotropic effect induced by a relatively modest (23% to 27%) degree of NCX block in both N and F. Frequency-dependent acceleration of relaxation has been shown to function in the failing hearts<sup>25</sup> and may represent an attractive inotropic target by itself.

### Effect of XIP in Failing Heart Cells

Because the balance between  $\text{Ca}^{2+}$  removal mechanisms is shifted toward more NCX-mediated  $\text{Ca}^{2+}$  extrusion in myocytes from failing hearts,<sup>8</sup> one would expect that the same degree of NCX block would induce a more substantial increase in the  $[\text{Ca}^{2+}]_i$  transients of this group.



This was exactly what we observed: a 27% inhibition of the NCX (which, in failing cells, is enhanced to  $\approx 200\%$  of normal<sup>2</sup>) induced a 3.86-fold increase in the  $[Ca^{2+}]_i$  transient amplitude (Figure 2c).

Importantly, despite impaired basal SERCA function, the myocytes from failing hearts were able to autoregulate  $[Ca^{2+}]_i$  in response to NCX inhibition by taking up and releasing more SR  $Ca^{2+}$ . Turning this argument around, one may speculate that the substantially lower ( $\approx 50\%$  of normal) basal SR  $Ca^{2+}$  uptake rate in heart failure<sup>8</sup> (Figure 6f), with only a 28% downregulation of pump protein,<sup>8</sup> may be partially caused by the lower amplitude  $Ca^{2+}$  transients and the lack of  $Ca^{2+}$  stimulation. There may be a vicious cycle between decreased SR  $Ca^{2+}$  release and uptake in heart failure, which was interrupted by XIP. Analogously, the robust stimulation of SERCA activity by  $\beta$ -adrenergic stimulation in failing myocytes<sup>8</sup> implies a low basal SERCA activity, but sufficient recruitable reserve capacity. The present findings motivate renewed efforts toward identifying the messenger involved in the  $Ca^{2+}$ -dependent stimulation of SERCA to clarify its therapeutic potential in heart failure.

### Experimental Assumptions and Limitations

The model used here has historically generated many insights into the physiopathology of heart failure.<sup>9</sup> From the point of view of cellular  $Ca^{2+}$  handling, canine (as well as rabbit and guinea pig) myocytes resemble human cells, with 70% reliance on SERCA for  $Ca^{2+}$  decay, and 25% on NCX. This differs from small rodent species, such as rats and mice, in which NCX plays a lesser role.<sup>26</sup> Hence, the effect of XIP may be substantially different in these animal models. The pacing-induced heart failure model resembles the human failing phenotype, with unchanged  $I_{Ca,L}$ , increased NCX, and decreased SERCA. One difference, however, is that we have not observed an elevation of the diastolic levels of  $[Ca^{2+}]_i$  in F versus N, which may be true in humans with end-stage heart failure. Therefore, one must be cautious about extrapolating the results to the human disease without further investigation.

The substantial increase in the  $[Ca^{2+}]_i$  transient in F suggested that XIP had a significant effect in these cells, but the caffeine-induced  $Ca^{2+}$  responses retained fast  $[Ca^{2+}]_i$  decay kinetics and large inward NCX currents (Figure 1c and 1d). This apparent inconsistency begged the question of how much NCX was inhibited in these experiments. With alternative methods, we found that 30  $\mu\text{mol/L}$  XIP inhibited NCX by 67% when  $Ca^{2+}$  was buffered to 112 nmol/L, and 27% when  $Ca^{2+}$  was allowed to oscillate freely between  $\approx 300$  and 500 nmol/L, suggesting that the apparent lack of effect of XIP in the presence of caffeine could be caused by the very high intracellular free  $Ca^{2+}$  concentrations reducing the effectiveness of the inhibitor. An alternative possibility is that the caffeine itself could be altering the extent of XIP block of the  $Na^+/Ca^{2+}$  exchanger, either directly or indirectly (eg, through its inhibition of phosphodiesterase activity). With respect to the notion that XIP inhibition could be diminished at high  $[Ca^{2+}]_i$ , it may be noted that the allosteric  $Ca^{2+}$  binding sites and putative XIP interaction domains lie near each other on the large intracellular loop region of NCX,<sup>27</sup> although competition between  $Ca^{2+}$  and XIP has not been observed in more isolated assay systems.<sup>14</sup> Thus, further studies will be required to validate this hypothesis. If it proves true, however, this effect would constitute an additional safeguard against XIP inducing  $Ca^{2+}$  overload by excessive inhibition of  $Na^+/Ca^{2+}$  exchange.

Another important issue is that the overall contribution of NCX to  $Ca^{2+}$  handling, and the effect of XIP documented here, is likely to be modulated by a number of cellular parameters *in vivo*. One is the specific contribution to the cellular  $Ca_i$  transients of  $Ca^{2+}$  entry via reverse-mode NCX during the action potential. The overall effect of NCX inhibition would represent the balance between an increase in SR  $Ca^{2+}$  release and a decrease in NCX mediated  $Ca^{2+}$  entry.  $Ca^{2+}$  entry through NCX is relatively more important in F<sup>20</sup>, so this effect may account for the somewhat smaller (but still significant) effect of XIP on  $Ca^{2+}$  transients evoked by action

potentials versus those evoked by voltage-clamp pulses. A second consideration is that intracellular  $\text{Na}^+$  levels have been reported to be increased in failing hearts,<sup>28</sup> and this may have an impact on the effects of NCX inhibition in vivo, when  $\text{Na}^+_i$  is not controlled by the experimental conditions.

### Therapeutic Relevance

The present findings suggest that NCX inhibitors may represent a new class of positive inotropic drugs in the treatment of congestive heart failure. Even in the absence of novel drug development, improvements in gene transfer technology in the near future may make myocyte-targeted XIP expression a feasible therapy. For the goals of this study, the NCX inhibitor was selective and mode-independent, but the positive inotropic effect could, theoretically, be facilitated by a preponderantly forward-mode NCX inhibitor and/or by block of PMCA (a lesser component of total  $\text{Ca}^{2+}$  efflux).

For clinical use, other possible effects of NCX inhibitors (on arrhythmogenesis, ischemia-reperfusion injury, etc) are in need of further investigation. While this is beyond the scope of the present article, it is worth noting that NCX inhibition will have both direct and indirect (ie, via the increase in  $\text{Ca}_{\text{SR}}$ ) effects, which sometimes may be contradictory. One example is the pro-arrhythmic mechanism involving delayed after-depolarizations. Increased  $\text{Ca}_{\text{SR}}$  (for example, in response to sympathetic overdrive) may predispose the heart to spontaneous SR  $\text{Ca}^{2+}$  release events, and trigger delayed after-depolarizations as a result of forward-mode NCX current.<sup>29</sup> In this case, NCX inhibition would be protective by decreasing the peak amplitude of the transient inward ( $I_{\text{ti}}$ ) current evoked by a spontaneous  $\text{Ca}^{2+}$  release. A similar point can be made about the effect of NCX inhibition on the action potential duration (another pro-arrhythmogenic mechanism). While XIP increased the duration of the action potential for stimuli evoking a similarly-sized  $[\text{Ca}^{2+}]_i$  transient,<sup>30</sup> the XIP-induced enhancement of SR  $\text{Ca}^{2+}$  release shortens the action potential at steady-state, as a consequence of  $\text{Ca}^{2+}$  feedback on the action potential waveform. A protective effect against ischemia-reperfusion injury would also be expected in the presence of an NCX inhibitor.<sup>31</sup>

In summary, the present results argue that partial inhibition of NCX is a powerful method for restoring excitation–contraction coupling in heart failure. This effect is brought about by an improvement of SR  $\text{Ca}^{2+}$  load and facilitation of the pulse-dependent positive  $\text{Ca}^{2+}$  staircase caused by a reduction in the amount of  $\text{Ca}^{2+}$  “stolen” from the cell on each beat by NCX. Secondary  $\text{Ca}^{2+}$ -dependent stimulation of the SR  $\text{Ca}^{2+}$  ATPase rate plays an additional important role in preventing diastolic  $[\text{Ca}^{2+}]_i$  overload. This study identifies NCX inhibition as a potential therapeutic strategy in congestive heart failure, a disease in which no effective long-term treatment is available, and offers a platform for the development of a new class of positive inotropic drugs. Finally, this study uncovers the importance of SR  $\text{Ca}^{2+}$  ATPase activation by  $[\text{Ca}^{2+}]_i$ , whose recruitment acts synergistically with NCX block to increase both  $\text{Ca}^{2+}$  release and removal, normalizing both sides of the contractile deficit in heart failure.

### Supplementary Material

Refer to Web version on PubMed Central for supplementary material.

### Acknowledgments

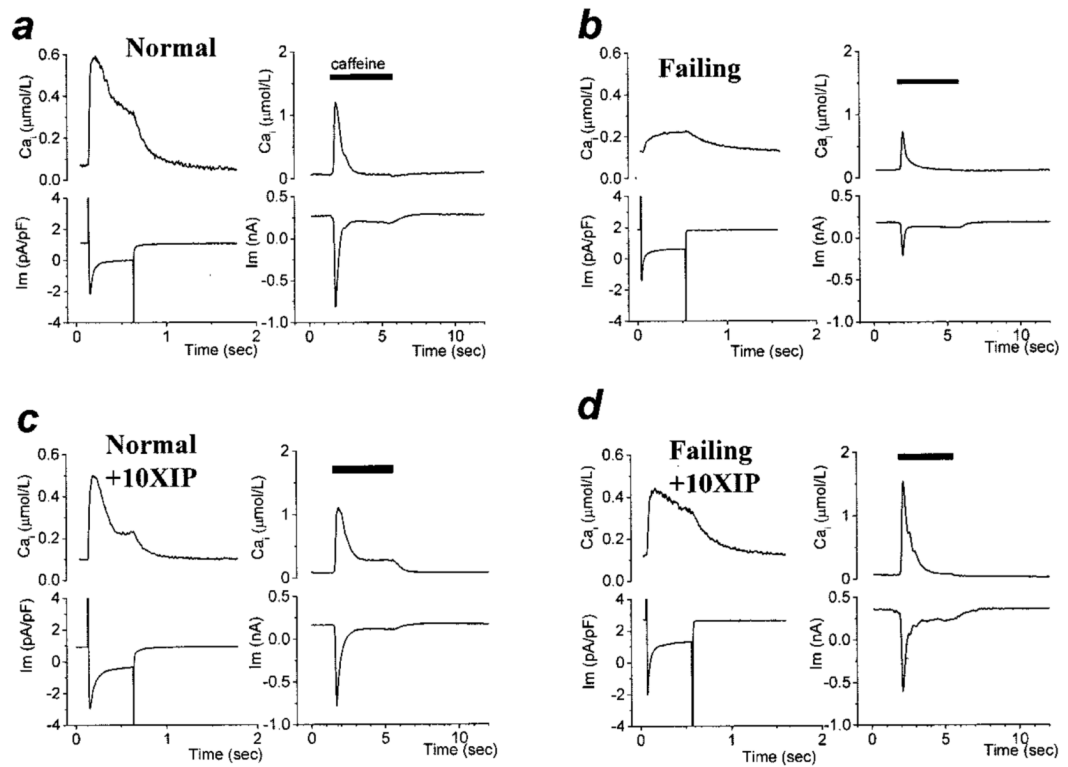
This work was supported by NIH R01HL61711 (B.O.), by the Specialized Center of Research on Sudden Cardiac Death in Heart Failure NIH P50 HL52307, and by an AHA postdoctoral fellowship (I.A.H.). C.M. was supported by the Deutsche Forschungsgemeinschaft (Emmy Noether Program). We acknowledge Eduardo Marbán, David Kass, and Gordon Tomaselli for helpful discussions, and Richard Tunin and Antonis Aroundas for help with dog preparation and surgery.

## References

1. Studer R, Reinecke H, Bilger J, Eschenhagen T, Böhm M, Hasenfuss G, Just H, Holtz J, Drexler H. Gene expression of the cardiac Na<sup>+</sup>-Ca<sup>2+</sup> exchanger in end-stage human heart failure. *Circ Res* 1994;75:443–453. [PubMed: 8062418]
2. Hobai IA, O'Rourke B. Enhanced Ca<sup>2+</sup>-activated Na<sup>+</sup>-Ca<sup>2+</sup> exchange activity in canine pacing-induced heart failure. *Circ Res* 2000;87:690–698. [PubMed: 11029405]
3. Pogwizd SM, Qi M, Yuan W, Samarel AM, Bers DM. Upregulation of Na<sup>+</sup>/Ca<sup>2+</sup> exchanger expression and function in an arrhythmogenic rabbit model of heart failure. *Circ Res* 1999;85:1009–1019. [PubMed: 10571531]
4. Hasenfuss G, Schillinger W, Lehnart SE, Preuss M, Pieske B, Maier LS, Prestle J, Minami K, Just H. Relationship between Na<sup>+</sup>-Ca<sup>2+</sup>-exchanger protein levels and diastolic function of failing human myocardium. *Circulation* 1999;99:641–648. [PubMed: 9950661]
5. Terracciano CM, Philipson KD, MacLeod KT. Overexpression of the Na<sup>+</sup>/Ca<sup>2+</sup> exchanger and inhibition of the sarcoplasmic reticulum Ca<sup>2+</sup>-ATPase in ventricular myocytes from transgenic mice. *Cardiovasc Res* 2001;49:38–47. [PubMed: 11121794]
6. Sipido KR, Volders PG, de Groot SH, Verdonck F, Van de Werf F, Wellens HJ, Vos MA. Enhanced Ca<sup>2+</sup> release and Na/Ca exchange activity in hypertrophied canine ventricular myocytes: potential link between contractile adaptation and arrhythmogenesis. *Circulation* 2000;102:2137–2144. [PubMed: 11044433]
7. Hobai IA, O'Rourke B. Decreased sarcoplasmic reticulum calcium content is responsible for defective excitation-contraction coupling in canine heart failure. *Circulation* 2001;103:1577–1584. [PubMed: 11257088]
8. O'Rourke B, Kass DA, Tomaselli GF, Kaääb S, Tunin R, Marbán E. Mechanisms of altered excitation-contraction coupling in canine tachycardia-induced heart failure, I: experimental studies. *Circ Res* 1999;84:562–570. [PubMed: 10082478]
9. Spinale, F. Pathophysiology of tachycardia-induced heart failure. Futura Publishing Company, Inc; Armonk, NY: 1996.
10. Watano T, Kimura J, Morita T, Nakanishi H. A novel antagonist, No. 7943, of the Na<sup>+</sup>/Ca<sup>2+</sup> exchange current in guinea-pig cardiac ventricular cells. *Br J Pharmacol* 1996;119:555–563. [PubMed: 8894178]
11. Tanaka H, Nishimaru K, Aikawa T, Hirayama W, Tanaka Y, Shigenobu K. Effect of SEA0400, a novel inhibitor of sodium-calcium exchanger, on myocardial ionic currents. *Br J Pharmacol* 2002;135:1096–1100. [PubMed: 11877314]
12. Hobai IA, Bates JA, Howarth FC, Levi AJ. Inhibition by external Cd<sup>2+</sup> of Na/Ca exchange and L-type Ca channel in rabbit ventricular myocytes. *Am J Physiol* 1997;272:H2164–72. [PubMed: 9176282]
13. Reuter H, Henderson SA, Han T, Matsuda T, Baba A, Ross RS, Goldhaber JI, Philipson KD. Knockout mice for pharmacological screening: testing the specificity of Na<sup>+</sup>-Ca<sup>2+</sup> exchange inhibitors. *Circ Res* 2002;91:90–92. [PubMed: 12142340]
14. Li Z, Nicoll DA, Collins A, Hilgemann DW, Filoteo AG, Penniston JT, Weiss JN, Tomich JM, Philipson KD. Identification of a peptide inhibitor of the cardiac sarcolemmal Na<sup>+</sup>-Ca<sup>2+</sup> exchanger. *J Biol Chem* 1991;266:1014–1020. [PubMed: 1985930]
15. Chin TK, Spitzer KW, Philipson KD, Bridge JH. The effect of exchanger inhibitory peptide (XIP) on sodium-calcium exchange current in guinea pig ventricular cells. *Circ Res* 1993;72:497–503. [PubMed: 8431979]
16. Schouten VJ. Interval dependence of force and twitch duration in rat heart explained by Ca<sup>2+</sup> pump inactivation in sarcoplasmic reticulum. *J Physiol* 1990;431:427–444. [PubMed: 2100313]
17. Bassani RA, Mattiazzi A, Bers DM. CaMKII is responsible for activity-dependent acceleration of relaxation in rat ventricular myocytes. *Am J Physiol* 1995;268:H703–H712. [PubMed: 7864197]
18. Enyedi A, Penniston JT. Autoinhibitory domains of various Ca<sup>2+</sup> transporters cross-react. *J Biol Chem* 1993;268:17120–17125. [PubMed: 8394328]

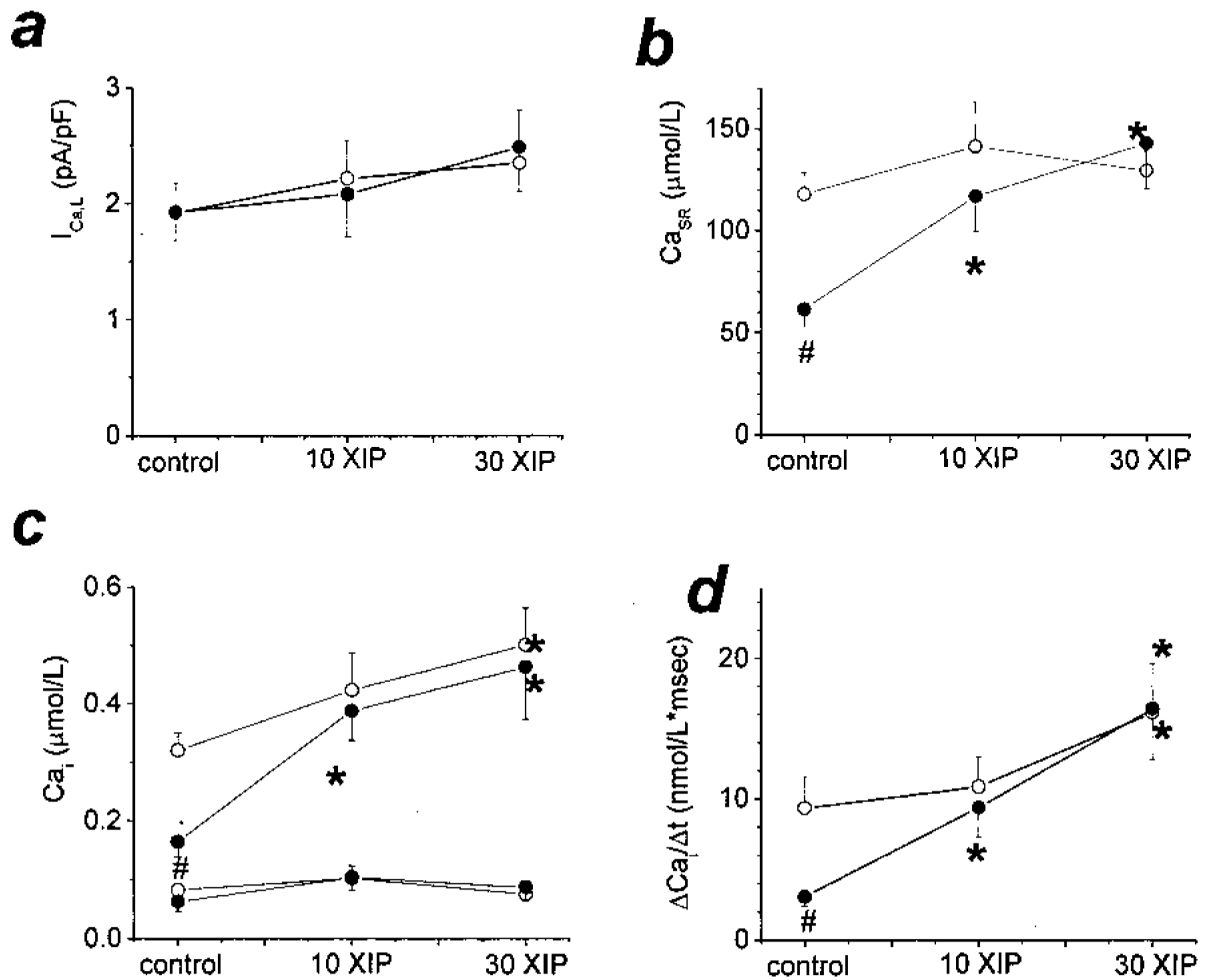


19. Bassani RA, Bassani JW, Bers DM. Mitochondrial and sarcolemmal  $\text{Ca}^{2+}$  transport reduce  $[\text{Ca}^{2+}]_i$  during caffeine contractures in rabbit cardiac myocytes. *Journal of Physiology* 1992;453:591–608. [PubMed: 1464847]
20. Dipla K, Mattiello JA, Margulies KB, Jeevanandam V, Houser SR. The sarcoplasmic reticulum and the  $\text{Na}^+/\text{Ca}^{2+}$  exchanger both contribute to the  $\text{Ca}^{2+}$  transient of failing human ventricular myocytes. *Circ Res* 1999;84:435–444. [PubMed: 10066678]
21. Weber CR, Piacentino V 3rd, Houser SR, Bers DM. Dynamic regulation of sodium/calcium exchange function in human heart failure. *Circulation* 2003;108:2224–2229. [PubMed: 14557358]
22. Eisner DA, Trafford AW, Diaz ME, Overend CL, O'Neill SC. The control of Ca release from the cardiac sarcoplasmic reticulum: regulation versus autoregulation. *Cardiovasc Res* 1998;38:589–604. [PubMed: 9747428]
23. DeSantiago J, Maier LS, Bers DM. Frequency-dependent acceleration of relaxation in the heart depends on CaMKII, but not phospholamban. *J Mol Cell Cardiol* 2002;34:975–984. [PubMed: 12234767]
24. Kassiri Z, Myers R, Kaprielian R, Banijamali HS, Backx PH. Rate-dependent changes of twitch force duration in rat cardiac trabeculae: a property of the contractile system. *J Physiol* 2000;524:221–231. [PubMed: 10747194]
25. Pieske B, Kretschmann B, Meyer M, Holubarsch C, Weirich J, Posival H, Minami K, Just H, Hasenfuss G. Alterations in intracellular calcium handling associated with the inverse force-frequency relation in human dilated cardiomyopathy. *Circulation* 1995;92:1169–1178. [PubMed: 7648662]
26. Bers, DM. *Excitation-Contraction Coupling and Cardiac Contractile Force*. Kluwer Academic Publishers; Dordrecht, The Netherlands: 2001.
27. Matsuoka S, Nicoll DA, Reilly RF, Hilgemann DW, Philipson KD. Initial localization of regulatory regions of the cardiac sarcolemmal  $\text{Na}^+/\text{Ca}^{2+}$  exchanger. *Proc Natl Acad Sci U S A* 1993;90:3870–3874. [PubMed: 8483905]
28. Despa S, Islam MA, Weber CR, Pogwizd SM, Bers DM. Intracellular  $\text{Na}^+$  concentration is elevated in heart failure but Na/K pump function is unchanged. *Circulation* 2002;105:2543–2548. [PubMed: 12034663]
29. Pogwizd SM, Schlotthauer K, Li L, Yuan W, Bers DM. Arrhythmogenesis and contractile dysfunction in heart failure: Roles of sodium-calcium exchange, inward rectifier potassium current, and residual beta-adrenergic responsiveness. *Circ Res* 2001;88:1159–1167. [PubMed: 11397782]
30. Armondas AA, Hobai IA, Tomaselli GF, Winslow RL, O'Rourke B. Role of sodium-calcium exchanger in modulating the action potential of ventricular myocytes from normal and failing hearts. *Circ Res* 2003;93:46–53. [PubMed: 12805237]
31. Magee WP, Deshmukh G, Deninno MP, Sutt JC, Chapman JG, Tracey WR. Differing cardioprotective efficacy of the  $\text{Na}^+/\text{Ca}^{2+}$  exchanger inhibitors SEA0400 and KB-R7943. *Am J Physiol Heart Circ Physiol* 2003;284:H903–H910. [PubMed: 12446284]



**Figure 1.**

XIP effects on  $\text{Ca}^{2+}$ -induced  $\text{Ca}^{2+}$  release. Square voltage clamp pulses ( $-80$  to  $+10$  mV,  $0.5$  s, at  $0.5$  Hz) were applied to isolated cardiac cells. After the  $\text{Ca}_i$  transients reached steady-state, the train of depolarizations was stopped and caffeine was applied to measure  $\text{Ca}_{\text{SR}}$ . a through d, Steady-state membrane currents and  $[\text{Ca}^{2+}]_i$  transients triggered by membrane depolarization (left) and the effect of caffeine (right) in myocytes from normal (N) or failing (F) hearts in the absence (a and b) or presence of  $10 \mu\text{mol/L}$  XIP (c and d) in the intracellular solution.

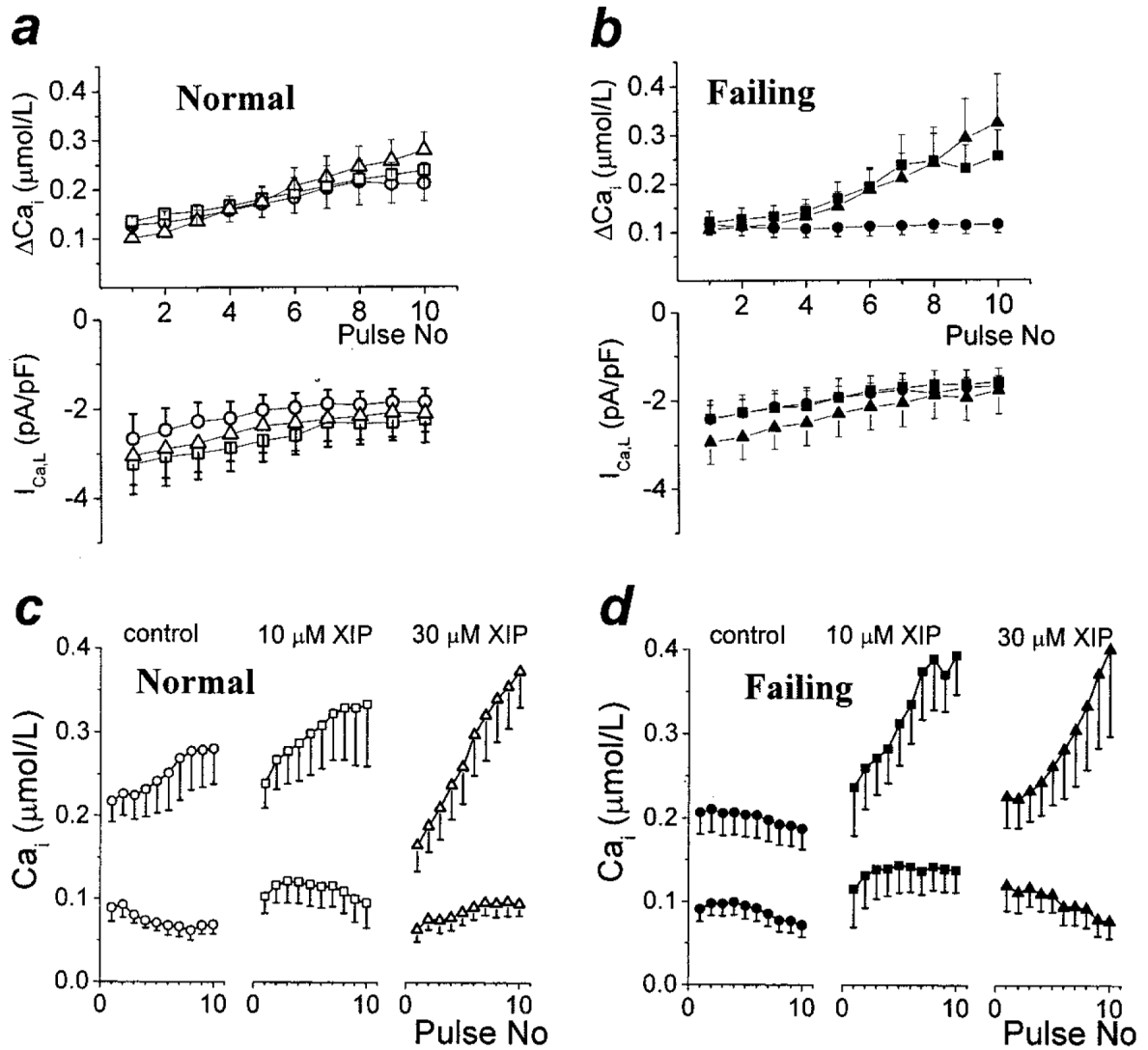


**Figure 2.**

XIP effects on  $\text{Ca}^{2+}$ -induced  $\text{Ca}^{2+}$  release. Average steady-state peak inward  $I_{\text{Ca,L}}$  (a),  $\text{Ca}_{\text{SR}}$  (as  $\mu\text{mol Ca}^{2+}$  stored in the SR per total cell volume [b]), diastolic and peak systolic  $[\text{Ca}^{2+}]_i$

(c), and  $\Delta\text{Ca}/\Delta t$  (d) in N (○) and F (●), in the absence or presence of 10 or 30  $\mu\text{mol/L}$  XIP.  $I_{\text{Ca,L}}$  was similar in all 6 groups. At baseline, F cells had decreased  $[\text{Ca}^{2+}]_i$  transients and reduced  $\text{Ca}_{\text{SR}}$ , which were normalized by XIP at 10 or 30  $\mu\text{mol/L}$  concentrations without affecting diastolic  $[\text{Ca}^{2+}]_i$ . In control conditions,  $n=25$  cells from 8 dogs (25/8) in N and 10/4 for F. For 10  $\mu\text{mol/L}$  XIP,  $n=14/3$  and 10/5; and for 30  $\mu\text{mol/L}$  XIP  $n=15/4$  and 12/2 for N and F, respectively. # $P<0.05$  between N and F groups for the same experimental condition.

\* $P<0.05$  within a group for XIP treatment versus baseline.

**Figure 3.**

XIP effect on the  $Ca^{2+}$  staircase. After a caffeine-induced  $Ca^{2+}$  release, restarting the train of depolarizations induced gradually increasing cellular  $Ca^{2+}$  transients (ie, a positive staircase). a,  $[Ca^{2+}]_i$  transient amplitude and  $I_{Ca,L}$  for the first 10 depolarizations (at 0.5 Hz) after a caffeine application.  $[Ca^{2+}]_i$  transients increased gradually with pacing in N ( $\circ$ ) and this effect was slightly accelerated by 10 ( $\square$ ) and 30  $\mu\text{mol/L}$  ( $\Delta$ ) XIP. b, In contrast, the positive  $Ca^{2+}$  staircase was absent in F ( $\bullet$ ), but was restored by XIP (either 10,  $\blacksquare$ , or 30  $\mu\text{mol/L}$ ,  $\blacktriangle$ ). c and d, Both diastolic and peak  $[Ca^{2+}]_i$  are shown for the data presented in (a) and (b) ( $n=12/5$ ,  $10/3$ ,  $9/3$ , and  $11/4$ ,  $7/4$ ,  $7/2$  for N and F, in control and with 10 and 30  $\mu\text{mol/L}$  XIP, respectively). The positive inotropic effect of XIP occurred without an associated increase in diastolic  $[Ca^{2+}]_i$ .

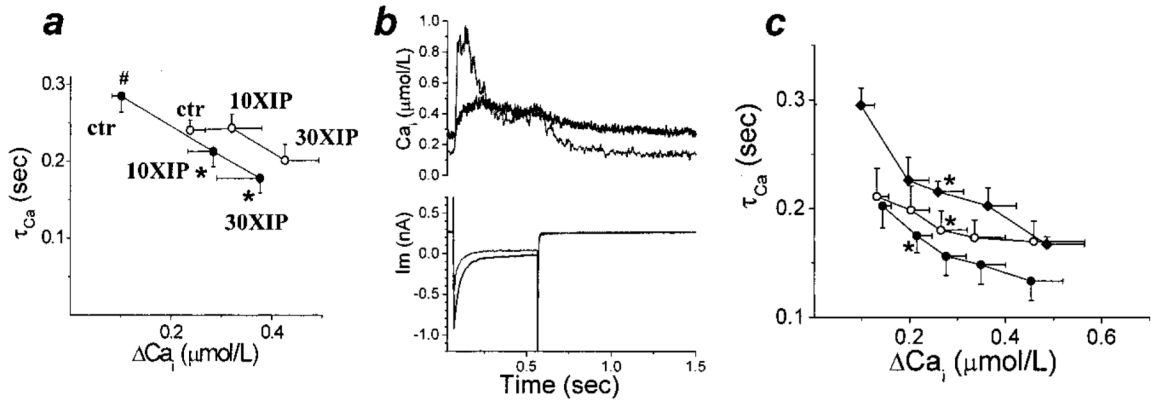


**Figure 4.**

XIP effects on  $[Ca^{2+}]_i$  decay. a, In control conditions, the time constant of  $Ca^{2+}$  decay ( $\tau_{Ca}$ ) was significantly longer in F compared with N ( $\#P < 0.05$ ). For the steady-state  $[Ca^{2+}]_i$  transients, XIP induced an unexpected acceleration of  $\tau_{Ca}$ , shown here in parallel with the increase in the amplitude of the  $[Ca^{2+}]_i$  transient ( $\circ$  N,  $\bullet$  F; n values as for Figure 1).  $\tau_{Ca}$  acceleration with XIP was significant in F only (\*), but evident for 30  $\mu\text{mol/L}$  XIP in N also. b, The relation between  $\tau_{Ca}$  and  $\Delta Ca$  was reproduced in individual cells during the development of the  $Ca^{2+}$  staircase (as in Figure 3). Typical traces exemplifying the decreased  $\tau_{Ca}$  associated with the increased  $[Ca^{2+}]_i$  transient at steady-state (light gray trace) vs first depolarization (black trace) after caffeine in F cell with 30  $\mu\text{mol/L}$  XIP. c, Average data for the experiments shown in (b). During the development of the staircase, we measured  $\tau_{Ca}$  of selected  $[Ca^{2+}]_i$  transients, which were equal to 150, 200, 250, and 300% of the first  $[Ca^{2+}]_i$  transient.  $\tau_{Ca}$  was then plotted as a function of  $\Delta Ca$ . In N ( $\circ$ ,  $n=6/4$ ) the increase in  $\Delta Ca$  was associated with a significant decrease in  $\tau_{Ca}$  (\*first data point whose  $\tau_{Ca}$  differed significantly from that of the initial  $Ca^{2+}$  transient). A similar result was seen in F when staircase developed with either 10 or 30  $\mu\text{mol/L}$  XIP ( $\bullet$ ,  $n=6/4$ ). A similar acceleration of  $\tau_{Ca}$  could also be observed in F in the absence of XIP when cells were superfused with 10 mmol/L  $Ca^{2+}$  Tyrode ( $\blacklozenge$ ,  $n=4/2$ ), suggesting that the abbreviation of  $\tau_{Ca}$  by XIP treatment was related to the increase in time-averaged  $Ca^{2+}$ .



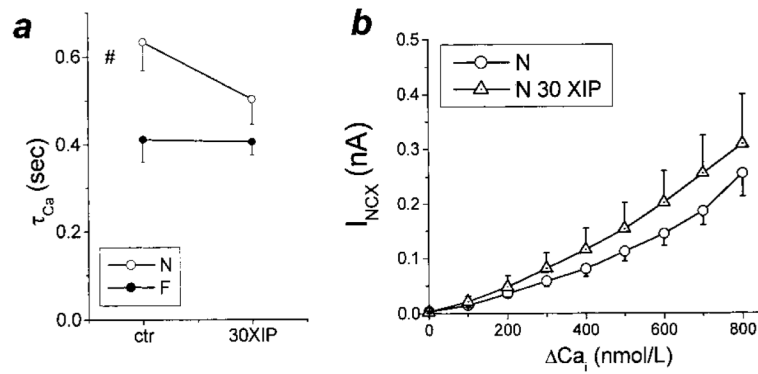


**Figure 5.** NCX activity during caffeine-induced  $Ca^{2+}$  release. a, The time constant ( $\tau_{Ca}$ ) of  $[Ca^{2+}]_i$  decay during caffeine is an index of NCX activity. Consistent with NCX overexpression in this model of heart failure,<sup>2</sup>  $\tau_{Ca}$  was significantly decreased in F versus N. However, XIP (30  $\mu$ mol/L) had no significant effect on  $\tau_{Ca}$  in either group. b, XIP also did not significantly alter the relationship between inward NCX current ( $I_{NCX}$ ) and  $\Delta Ca$  in either group (F data not shown). The steady-state current and  $[Ca^{2+}]_i$  in the presence of caffeine were used as baseline values in determining  $\Delta Ca$ .

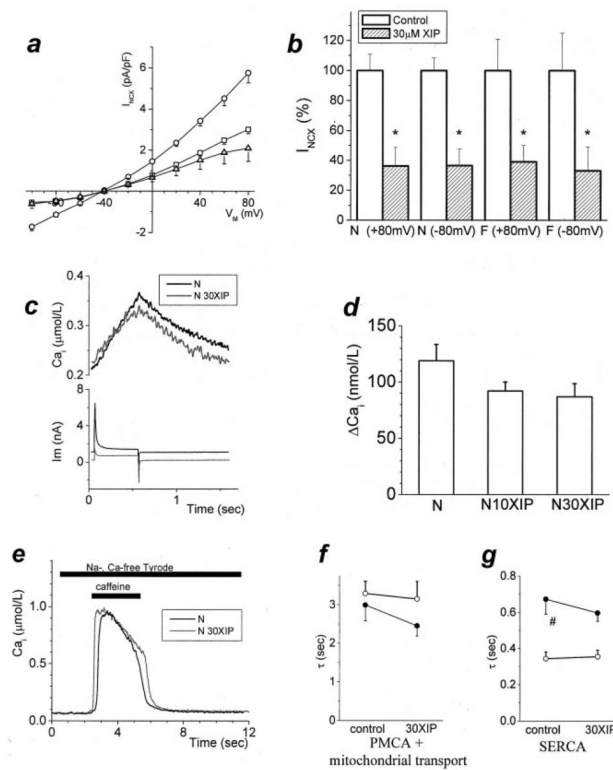


**Figure 6.**

Quantifying NCX block and selectivity. Additional methods were used to estimate the degree of NCX inhibition by XIP. a, NCX current was measured selectively<sup>2</sup> with  $[Ca^{2+}]_i$  buffered to 112 nmol/L (N,  $\circ$ ); 10 ( $\square$ ) and 30  $\mu$ mol/L ( $\Delta$ ) XIP inhibited NCX by 48% and 64%, respectively (at +80 mV). The degree of inhibition was similar over the entire range of test potentials;  $P < 0.05$  at all potentials except the reversal potential ( $n = 22/6, 6/2, 7/2$  for control, 10 and 30  $\mu$ mol/L XIP). b, The extent of inhibition by 30  $\mu$ mol/L XIP was similar in N and F groups for both forward (-80 mV) and reverse (+80 mV) modes of  $Na^+/Ca^{2+}$  exchange (mean  $\pm$  SEM, normalized to the average current in the absence of XIP). c, In N myocytes treated with 1  $\mu$ mol/L thapsigargin (conditions otherwise the same as in Figures 1 through 5), a depolarization from -80 mV to +100 mV induced reverse-mode NCX (typical traces shown for untreated conditions and 30  $\mu$ mol/L XIP). d, This NCX-induced  $[Ca^{2+}]_i$  increase was inhibited to 77% and 73% of baseline levels by 10 and 30  $\mu$ mol/L XIP, respectively (NS,  $n = 8/5, 5/2, 7/2$  for N in control and with 10 and 30  $\mu$ mol/L XIP, respectively). e through g, A separate experiment was performed to confirm that the XIP effect was not caused by nonspecific effects on other  $Ca^{2+}$  handling mechanisms. With the NCX inhibited by a  $Na^+$ -free,  $Ca^{2+}$ -free external solution, SR  $Ca^{2+}$  release was induced with caffeine. Conditioning pulse protocols were adjusted so that the size of the SR  $Ca^{2+}$  release was similar in all 4 experimental groups. During caffeine application, the only effective  $Ca^{2+}$  extrusion mechanisms are the plasmalemmal  $Ca^{2+}$  ATPase (PMCA) and mitochondrial  $Ca^{2+}$  uptake, whereas after caffeine removal, the SR  $Ca^{2+}$  pump also contributes to  $Ca^{2+}$  removal.<sup>19</sup> The time constants of  $Ca_i$  decay corresponding to PMCA and mitochondrial transport and SERCA were not changed in the presence of 30  $\mu$ mol/L XIP. e, Caffeine-evoked  $Ca^{2+}$  transients, in N untreated and with 30  $\mu$ mol/L XIP. f and g, Average data ( $n = 8/4$  and  $6/2$  for N and  $9/2$  and  $7/2$  for F, in control and with 30  $\mu$ mol/L XIP, respectively;  $P = NS$ ). Under control conditions,  $\tau_{Ca}$  corresponding to SERCA was significantly slower in F ( $\#P < 0.05$ ), as expected.

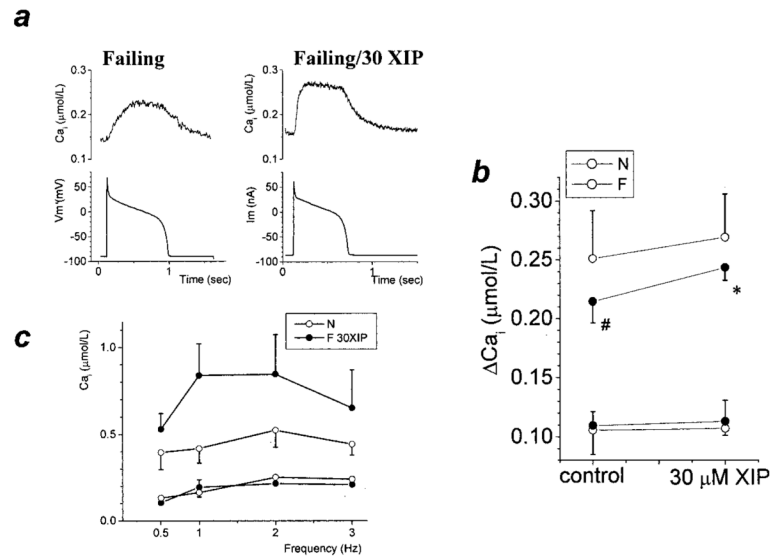


**Figure 7.**

The effect of XIP in various conditions. a, Typical action potential-driven Ca<sub>i</sub> transients showing the effect of 30 μmol/L XIP in F. b, Both diastolic and peak systolic [Ca<sup>2+</sup>]<sub>i</sub> are shown for each group. Steady-state action potential driven Ca<sub>i</sub> transients (0.25Hz) were significantly smaller in F versus N; 30 μmol/L XIP significantly increased the Ca<sub>i</sub> transients in F and a similar trend was evident in N (N: n=9/3 and 5/2; F: n=8/4 and 4/2 for control or 30 μmol/L XIP, respectively). ○, N; ●, F. c, Steady-state diastolic and peak systolic [Ca<sup>2+</sup>]<sub>i</sub> in untreated N cells (n=5/2) and F cells with 30 μmol/L XIP (n=4/2) paced between 0.5 and 3Hz (voltage-clamp mode; duration of pulse depolarization 100 ms). The increase in diastolic [Ca<sup>2+</sup>]<sub>i</sub> at higher frequencies was minor and similar in N and F cells with XIP.